Chapter 12

Mesoscale Imaging of Stroke

Adam Santorelli, Colin T. Sullender, Christopher Smith, and Andrew K. Dunn

Abstract

Preclinical research allows neuroscientists and engineers to investigate both physiological effects of stroke and the subsequent recovery, as well as design, test, and optimize novel imaging methods and devices. Anesthesia is widely used to help sedate animals; however, the use of anesthesia has been shown have systemic effects on neuronal and vascular function. Thus, awake imaging in rodents has gained popularity. Specifically, awake imaging for stroke enables a better understanding of the process of ischemic stroke formation, the mechanisms of neuronal death, and the subsequent recovery period. In this protocol, we provide a guide on the development of a laser speckle contrast imaging system that allows for the implementation of a novel dual-modality system that allows for awake imaging and a targeted photothrombosis method. Laser speckle contrast imaging (LSCI) is a label-free optical imaging technique that can provide continuous full-field images of the blood flow dynamics of the cortical surface. We harness this technique to provide continuous monitoring of the vasculature of the cortex to allow for user-defined targeted regions for photothrombosis in awake mice. Furthermore, we show how the system can be used for chronic awake imaging of stroke mice to assess the revascularization of the infarct region.

Key words Cerebral blood flow, Optical imaging, Laser speckle contrast imaging, Multi-exposure speckle imaging, Neurosurgery, Awake stroke imaging

1 Introduction

The transition to fully awake imaging eliminates the systemic effects of general anesthesia. Anesthesia is widely used in preclinical neuroscience research to sedate animals while imaging despite systemic effects on neuronal and vascular function [1]. Isoflurane has been shown to reduce excitatory synaptic transmission [2], impair oxygen autoregulation [3], suppress the magnitude and speed of neurovascular coupling [4], and cause abnormal increases in cerebral blood flow (CBF) [5, 6]. Isoflurane has also been shown to convey neuroprotective effects that may reduce the severity of ischemic lesions [7, 8] and suppress the occurrence and frequency of spreading depolarizations [9]. These effects can mask the benefits of

James E. Niemeyer et al. (eds.), *Awake Behaving Mesoscopic Brain Imaging*, Neuromethods, vol. 214,
https://doi.org/10.1007/978-1-0716-4120-0_12,

neuroprotective agents and potentially impact the outcomes of long-term studies [10, 11]. Additionally, the use of different general anesthetics (urethane vs. isoflurane) can lead to conflicting vascular measurements [12–14].

Laser speckle contrast imaging (LSCI) is a full-field, label-free, optical imaging technique that can provide continuous maps of blood flow; thus, it can be used in an extensive number of applications across neuroscience, dermatology, dentistry, and ophthalmology [15, 16]. Studies have covered research topics such as monitoring CBF during ischemic stroke induction [17], chronic monitoring of the vasculature remodeling after stroke induction [9, 18, 19], investigating the effects of isoflurane-based vasodilation [20], and studying the impact of obesity on CBF [21]. There have also been advancements in research to integrate speckle contrast measurements within a surgical microscope for intraoperative use [22, 23].

Multi-exposure speckle imaging (MESI) was developed as an extension of LSCI to provide a more robust estimate of the correlation time constant (τ_c), ultimately allowing for accurate chronic monitoring of vascular blood flow. MESI requires collecting LSCI images over a wide range of camera exposure times to properly sample the underlying flow dynamics. While the complexity of the MESI hardware has been challenging to integrate into a clinical setting [23], MESI has been used for a wide array of in vivo mouse studies. MESI can create flow maps, commonly using the Inverse Correlation Time (ICT, $1/\tau_c$) as a quantifiable metric to represent flow, thus creating ICT maps, over the entire region of interest (ROI) that is being imaged. MESI is noninvasive (once a cranial window has been implanted), and does not require any dye injection, thus we are able to perform continuous imaging both during the stroke induction and any chronic imaging during the subsequent recovery period, the repeated measurements do not induce any unneeded stress on the mouse.

Animal models of ischemic stroke are extensively used to study the mechanisms of neuronal death and recovery and to perform preliminary testing on neuroprotective interventions. While there are numerous techniques for inducing focal ischemia, the majority rely upon occlusion of the middle cerebral artery (MCA) and its branches. The MCA is the largest cerebral artery in the brain and the most common vessel involved with human ischemic events [24]. The models that can most reliably reproduce the lesions and pathophysiology of human stroke (e.g. ischemic core and penumbra) offer the best experimental platforms for preclinical research.

Intraluminal MCA occlusion (MCAo) is the most widely used technique and is performed by introducing a monofilament suture into the internal carotid artery to block blood flow to the MCA [25]. This model is capable of inducing both permanent and transient focal ischemia similar to that of human stroke and does not

require craniotomy. The procedure results in large-scale infarct volumes (21–45% of ipsilateral hemisphere) that most closely resemble malignant infarction in humans [26]. However, the majority of human strokes are much smaller in size (4.5–14%) [26, 27], making traditional MCAo a poor model for studying recovery at a similar scale.

The photothrombosis model of stroke induction uses intravascular photooxidation to generate well-defined cortical lesions [28]. Photosensitive dyes such as rose bengal are injected intravenously and irradiated with light to produce singlet oxygen, which causes localized endothelial damage initiating platelet aggregation and thrombus formation [29]. Rose bengal has been extensively utilized as a photothrombotic agent [30, 31] and has well-characterized pharmacokinetics with fast clearance from the body [32]. A significant advantage of the photothrombotic model is the ability to stereotactically control the position and size of the infarct to target specific functional regions. However, the technique results in rapid vasogenic edema, which is thought to restrict the development of the ischemic penumbra and local reperfusion [26].

A digital micromirror device (DMD) is an optical semiconductor device that consists of a two-dimensional array of thousands of individually addressable mirrors that can be tilted to spatially modulate light. The DMD offers a new method for targeted photothrombosis that allows for increased control over the stroke induction process compared to conventional techniques that only illuminate a single focal volume. Entire vessels, arbitrarily shaped regions, or even multiple locations can be simultaneously occluded by using the DMD to pattern the irradiating light. By specifically targeting vessels, collateral photooxidative damage to the surrounding tissue can be minimized.

The elimination of anesthesia from neuroimaging experiments has grown increasingly popular in recent years with two primary strategies taking the forefront. The first is the use of head-mounted miniaturized components [33–35]. While this technique allows for freely moving tethered imaging, it requires extensive optical engineering, increasing the complexity and associated costs, additionally, it introduces significant motion artifacts caused by normal animal behavior [34]. The second strategy, which is implemented in this chapter, permits the use of existing imaging platforms and involves restraining the animal's head while positioned on a treadmill [4, 36–39] or confined in a small chamber [40]. This technique allows for walking or running in place while minimizing motion of the head and imaging region.

The procedure in this protocol can be summarized as follows; first, a chronic cranial window, with an attached headbar, must be implanted in the mouse subject; secondly, the imaging and targeted-stroke induction system must be modified to allow for awake imaging, this includes the integration of a low-profile

continuous belt treadmill and the optics required for the MESI system and DMD-targeted photothrombosis. Finally, we outline the process to simultaneously collect blood flow images from awake mice during the stroke induction, and the subsequent recovery period, including details for chronic imaging to assess recovery.

2 Materials

2.1 Cranial Window Implantation

1. Use medical air vaporized isoflurane (2.0%) via nose-cone inhalation to anesthetize the mouse.
2. Use a feedback heating pad (such as DC Temperature Controller, FHC) to maintain body temperature at 37 °C.
3. Monitor vital signs via pulse oximetry (MouseOx, Starr Life Sciences).
4. Place the mouse in a head-fixed stereotaxic frame (Narishige Scientific Instrument Lab) and administer carprofen (5 mg/kg, subcutaneous) for anti-inflammation and dexamethasone (2 mg/kg, intramuscular) to reduce the severity of cerebral edema following removal of the skull.
5. Sterilize all tools and the artificial cerebrospinal fluid (ACSF, buffered pH 7.4) in an autoclave.
6. Shave and resect the scalp to expose skull between the bregma and lambda cranial coordinates. Apply a thin layer of cyanoacrylate (Vetbond Tissue Adhesive, 3 M) to the exposed skull to facilitate the adhesion of dental cement.
7. Using a dental drill, (0.8 mm burr, Ideal Microdrill, Fine Science Tools) remove a 2–3 mm diameter portion of the skull over the frontoparietal cortex while leaving the dura intact. Ensure regular ACSF perfusion to prevent overheating.
8. Place a 5 mm round cover glass (#1.5, World Precision Instruments) over the exposed brain.
9. Deposit a dental cement mixture along the perimeter while applying gentle pressure to the cover glass. This process bonds the cover glass to the surrounding skull to create a sterile, air-tight seal around the craniotomy and allows for restoration of intracranial pressure.
10. Align the circular cutout in the headbar with the cranial window and rotate it laterally until parallel with the cover glass. This ensures that the cranial window will be perpendicular to the imaging system's optical axis when the animal is restrained in the awake imaging setup.
11. Apply dental cement around the headbar to permanently attach it to the animal's skull.

12. Apply a second layer of cyanoacrylate over the dental cement to further seal the cranial window (*see* **Note 1** for additional details).

2.2 Awake Imaging Treadmill System

The design of the awake imaging treadmill system is based on [39, 41], and allows for one-dimensional self-propelled movement. This low-profile system allows for ease of use with most optical systems designed in labs. Additionally, this system minimizes motion artifacts due to vertical variations that were encountered with the foam wheel treadmill design. The mouse was restrained by fixing the head plate into the holder.

Materials

1. Four 25 mm square optical construction rails (Thorlabs XE25L09).
2. Two ½″ diameter posts (Thorlabs TR12).
3. Two right-angle mounts for ½″ diameter rods (Thorlabs RA90).
4. Two ½″ diameter brass or steel rods to act as headplate bars (custom machined for holding headplate; schematic available at http://github.com/blinklab).
5. Two 2–56 screws for attaching headplate to brass rods.
6. One 1.5″ wide black polyester ribbon flat belt (Creative Ideas GRO1102-030).
7. Two sets of LEGO tires and axles (front and rear roller) that are 0.25″ and 0.375″ respectively.
8. Vero Black, for 3-D printing the main body (Janelia Labs, J005549 NRB Main Body schematic).

Construction

1. Form the base of the treadmill using four optical construction rails (Fig. 1), which allows for integration with the optical table and optical components.
2. Print the main body of the treadmill using a high-quality 3-D printer.
3. Screw the main body of the treadmill into the optical rail housing.
4. Integrate the LEGO tires and wheel with the main body of the treadmill.
5. Wrap the ribbon belt across the wheels to form the flat belt that will allow for self-propelled motion.

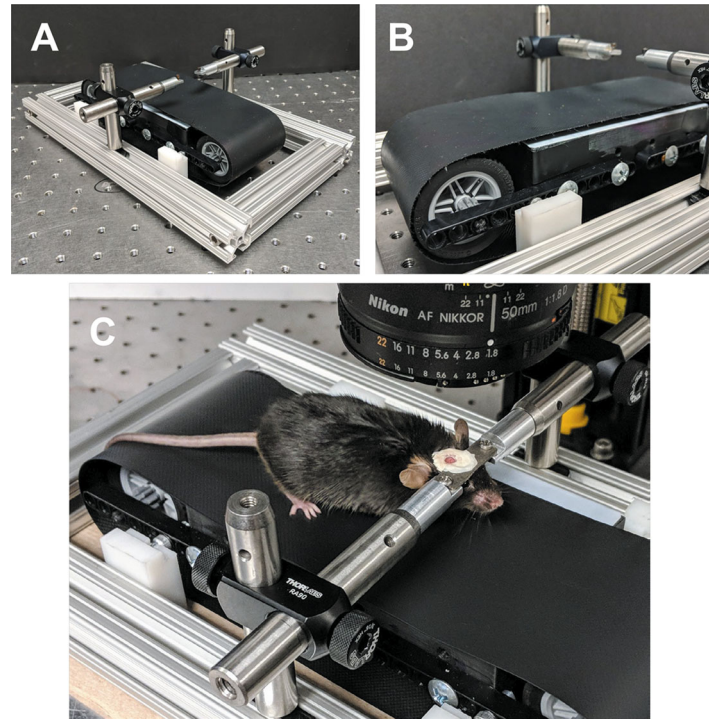

Fig. 1 Photographs of the awake imaging system showing the (**a**) low-profile, self-propelling belt treadmill, with (**b**) a close-up of the pulley system, and (**c**) a mouse placed under the optical imaging system with its head-restrained on the belt treadmill using the permanently attached headbar

6. Screw the two ½″ diameter Thorlabs posts into the optical rails, approximately centered over the midpoint of the treadmill.
7. Place one right-angle mount on each post, about 1½″ above the surface of the treadmill, so that the headplate bars can be passed through the mounts and meet above the treadmill. Adjust the right-angle mounts until the headplate bars can hold a headplate without straining the metal. Rotate the headplate bars so that they are at a known angle relative to the surface of the vibration isolation table. Also make sure that this angle will hold the mouse's head in a reasonable position (*see* **Note 2** for treadmill maintenance).

2.3 Optical Imaging Setup Requirements

A detailed explanation of the design, requirements, and implementation of the MESI system has been reported previously [42]. Here we include the modifications necessary for the targeted stroke induction (Fig. 2).

1. Stroke induction laser: Use a continuous wave green laser (typically 532 nm such as the 200 mW AixiZ LLC) to induce the targeted photothrombosis (when coupled with rose bengal

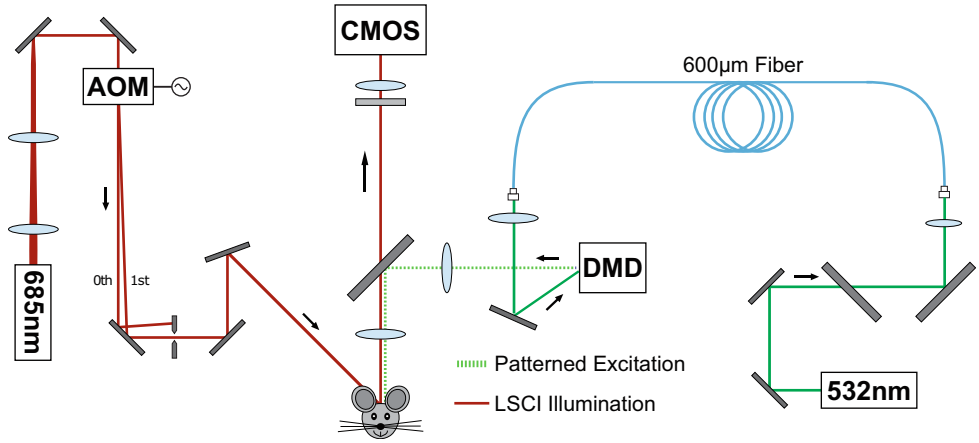

Fig. 2 A detailed schematic of the dual modality system that includes the MESI system and the DMD targeted stroke systems

dye). The packaged diode laser has a 2 mm collimated output that operates at a fixed current with convection cooling.

2. Use a neutral density filter (OD 1.0, NE10A-A, Thorlabs, Inc.) to attenuate the laser power. Usually only about 20 mW is needed.
3. Couple the green light into a fiber optic patch cord.
4. To relay the laser light, prior to creating the pattern, use a fiber optic patch cord with a 600 μm core size. This light will be used to illuminate the DMD.
5. A DLP® LightCrafter™ Evaluation Module (Texas Instruments Inc.) was modified to expose the bare DMD (DLP3000, 608 × 684 pixels, 7.6 μm pitch, Texas Instruments Inc.), *see* **Note 3**, for illumination. The spatially patterned modulated light was then relayed to the sample with 0.5× magnification.
6. Imaging light source: A wavelength-stabilized laser diode (ideally in the 600–850 nm wavelength range), capable of generating a decent amount of power, to ensure sufficient light at the shortest exposure time (ideally on the order of 50 μs), is the ideal choice of illumination for MESI (for example, 50 mW, HL6750MG, Thorlabs, Inc.).
7. Temperature-controlled housing: Mount the chosen laser diode in a laser diode mount with integrated temperature control (for example, TCLDM9, Thorlabs, Inc.).
8. Temperature controller: For stability and repeatability, use a temperature controller (TEC, such as TED200C, Thorlabs, Inc.) to set and maintain the laser diode operating temperature.

9. Laser diode controller: For the stability and repeatability of the illumination light, drive the laser diode with a constant current, controlled by a laser diode controller (such as the LDC202, Thorlabs, Inc.).
10. Light modulation: Use a free space AOM (for example, AOMO 3100-125, Gooch and Housego) and an RF driver (97-03307-34, Gooch and Housego) to modulate the intensity of the collimated laser light, ensuring the successful implementation of MESI. Use an iris to isolate the first order diffracted light from the free space AOM.
11. Field of view control: An aspheric lens (C240TME-B, Thorlabs, Inc.) can be used to control the beam diameter (here it was reduced to 1 mm).
12. Collection optics: The scattered light was relayed through a pair of dichroic beamsplitters and a bandpass filter (685 ± 40 nm, S685/40m, Chroma Technology Corp.). Use a pair of camera lenses (for example, 50 mm Nikon DSLR lenses) to direct the collected light to the camera sensor.
13. Camera: Use a high-speed CMOS camera that can be triggered from external source (such as the acA1920-155um Basler AG). The camera can be monochromatic, as only pixel intensity is required.
14. Control electronics: Use a multifunction I/O device (USB-6363, National Instruments Corp.), referred to as the data acquisition hardware (DAQ), to produce the camera exposure trigger signals and AOM modulation voltages. The drivers and associated libraries (NI-DAQmx library) for the DAQ will need to be installed (*see* **Note 4** for further details about MESI).
15. Processing software: Compute the speckle contrast, at each exposure time, from the collected raw signals. Solve the MESI equation, often using via nonlinear least squares curve fitting, to compute the ICT maps. These steps can easily be done in common post-processing software such as MATLAB.

3 Methods

3.1 Awake Imaging During Targeted Stroke Induction

This section will cover the steps necessary for awake imaging during targeted stroke induction. Note that the stroke induction procedure itself required the brief use of anesthesia for the injection of the photothrombotic agent. While it is unclear what minimum dosage of isoflurane is needed to convey its neuroprotective effects [10], the photothrombosis was performed under the lingering influence of isoflurane. This obfuscates the true changes in blood flow and oxygenation caused by the photothrombotic occlusion

itself. Transitioning to a tail vein or intraperitoneal injection prior to mounting on the treadmill would allow for the complete elimination of isoflurane from the stroke induction process. The resulting infarct was less severe than the anesthetized demonstration and was likely mitigated by the availability of collateral blood supply.

1. Initialize the dual modality system and ensure all optical components are functional and at a stable operating point.
2. The subject mouse is fixed to the headplate holder of the system (*see* **Note 5** for details about potential motion artifacts due to locomotion) as in Fig. 1. Allow several minutes for habituation.
3. Launch the speckle imaging software to ensure system functionality and that the cortical surface is in focus.
4. The subject was briefly anesthetized on the treadmill via nose-cone inhalation of isoflurane (3.0%).
5. Rose bengal was administered intravenously via retro-orbital injection (50 μL, 15 mg/mL).
6. Stop anesthesia and remove the nose-cone. The mouse will typically regain consciousness after about 3 min.
7. Check the live speckle image view to ensure that the cortical surface remains in focus after the dye injection.
8. Using the speckle software choose the specific region of interest (ROI) that will be illuminated by the patterned DMD light. This is the area that will undergo clot formation (*see* **Note 6** for additional details about DMD pattern control).
9. Expose the subject to the DMD-patterned green light for approximately 5–15 min to induce a photothrombotic occlusion. Descending arterioles were the primary targets because they serve as bottlenecks in the cortical oxygen supply. Target vessels were identified based on vascular orientation and a posteriori knowledge. After selecting a target vessel, adjust the subject such that the target vessel is approximately in the center of the FOV. This target area should also be the region of best focus if the surface is curved and consistent focus across the FOV is impossible.
10. Use the live speckle view in the software to monitor clot formation within the targeted area. An example of this process is shown in Fig. 3; details about this series of figures is described below. The series of speckle contrast images depict the progression of photothrombosis with the targeted vessel fully occluding after less than 3 min of exposure.
    (i) Images in Fig. 3a, b are the speckle contrast values over the entire FOV. Areas in black represent regions of low speckle contrast (high flow), whereas regions in white are indicative of no flow.

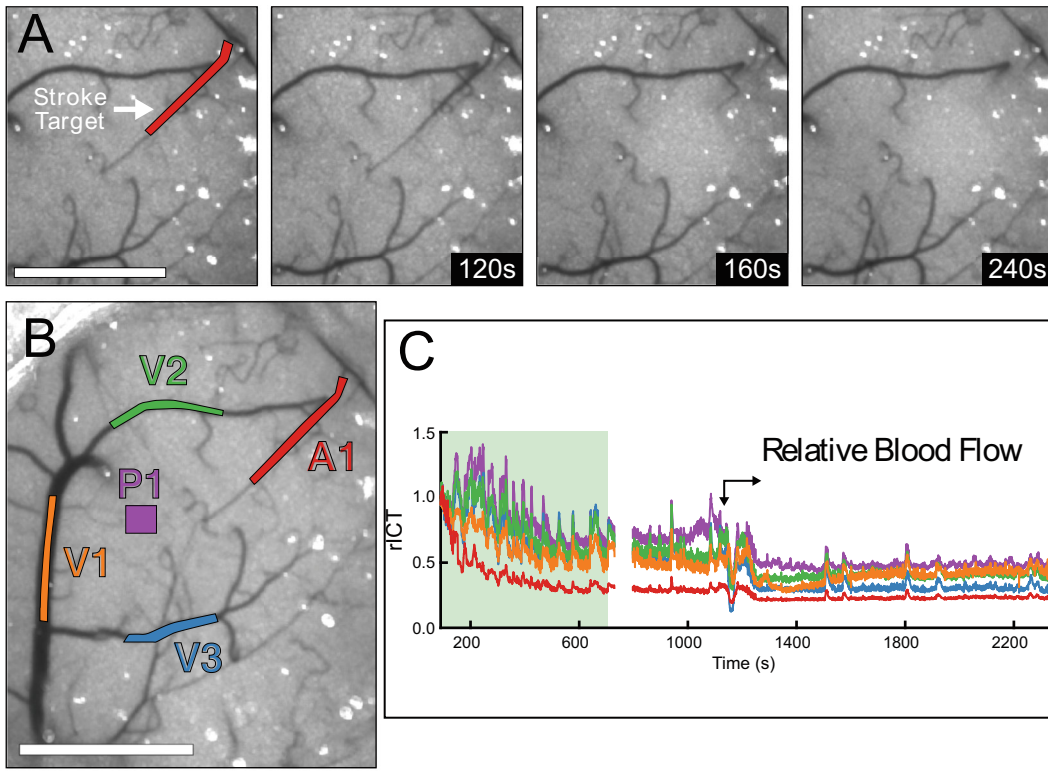

Fig. 3 (**a**) Single-exposure speckle contrast images depicting the occlusion of a descending arteriole using DMD-targeted photothrombosis. The red overlay indicates the 0.06 mm^2 region simultaneously illuminated for occlusion. (**b**) One arteriole (A1), three veins (V1, V2, V3), and one parenchyma region (P1) were targeted for flow measurements after stroke induction. (**c**) Relative blood flow within the targeted regions during and after photothrombosis. The green-shaded section indicates irradiation of the targeted arteriole. The gap in data occurred because of technical difficulties. The arrows indicate the propagation of an ischemia-induced depolarization event (White scale bars = 1 mm)

(ii) Figure 3a presents a series of speckle contrast images for the first 4 min post-photothrombosis (with the target vessel highlighted in red at $t = 0$ s). This time series of speckle images confirms the occlusion of the targeted vessel.

(iii) We highlight the five regions in Fig. 3b (one arteriole, three veins, and one parenchyma) we monitored for dynamic relative blood flow. The arteriole region (A1) is the same vessel targeted for photothrombotic occlusion. The resulting timecourses of relative blood flow (using the relative ICT values) can be seen in Fig. 3c. Compared to anesthetized photothrombosis measurements, these timecourses are significantly more variable because of walking and other animal motions. However, the subject had no visible reaction to the photothrombosis. By $t = 200$ s,

flow within the targeted arteriole had decreased to <50% of baseline. However, the animal was likely still experiencing the effects of anesthesia, making it impossible to attribute the changes exclusively to the photothrombotic occlusion.

(iv) The propagation of an ischemia-induced depolarization event can be seen beginning at $t = 1150$ s, with sharp reductions in relative blood flow across all ROIs. The magnitude of these changes are smaller than those seen in the anesthetized data [20], which is consistent with the results of a calcium imaging study performed during awake ischemic stroke [43]. As the depolarization subsided, flow within the targeted arteriole further decreased to <20% of baseline. Flow in all other regions remained depressed following the depolarization and were relatively steady until the end of the 40-min imaging session. There was also a reduction in animal motion compared to pre-depolarization behavior as seen by the lack of regular spikes in relative blood flow.

11. If stroke induction is not effected after 15 min, repeat the steps for injection and stroke injection to help the stroke take. This should not be repeated more than once at this dosage.

3.2 Chronic Awake Post-Stroke Hemodynamics

This section covers the monitoring of the chronic progression of the ischemic lesion using awake imaging for 8 days following photothrombosis, with the same mouse subject as in Subheading 3.1 (*see* **Note 7** for details on the upkeep of the mouse for chronic imaging). Anesthesia was not utilized in any of the post-photothrombosis imaging sessions. Data was only acquired when the animal was completely stationary because motion could interfere with the measurements and the resulting hemodynamic response would not be indicative of the resting state. Each imaging session followed the same protocol, namely:

1. Initialize the MESI imaging system (the DMD system is not needed for chronic awake imaging) and ensure all optical components are functional and at a stable operating point.
2. The subject mouse is fixed to the headplate holder of the system (*see* **Note 5** for details about potential motion artifacts due to locomotion) as in Fig. 1. Allow several minutes for habituation.
3. Launch the speckle imaging software to ensure system functionality and that the cortical surface is in focus.
4. Collect MESI sequences, typically, 1 min of data is sufficient.
5. Repeat the process for desired number of days/sessions in the study.

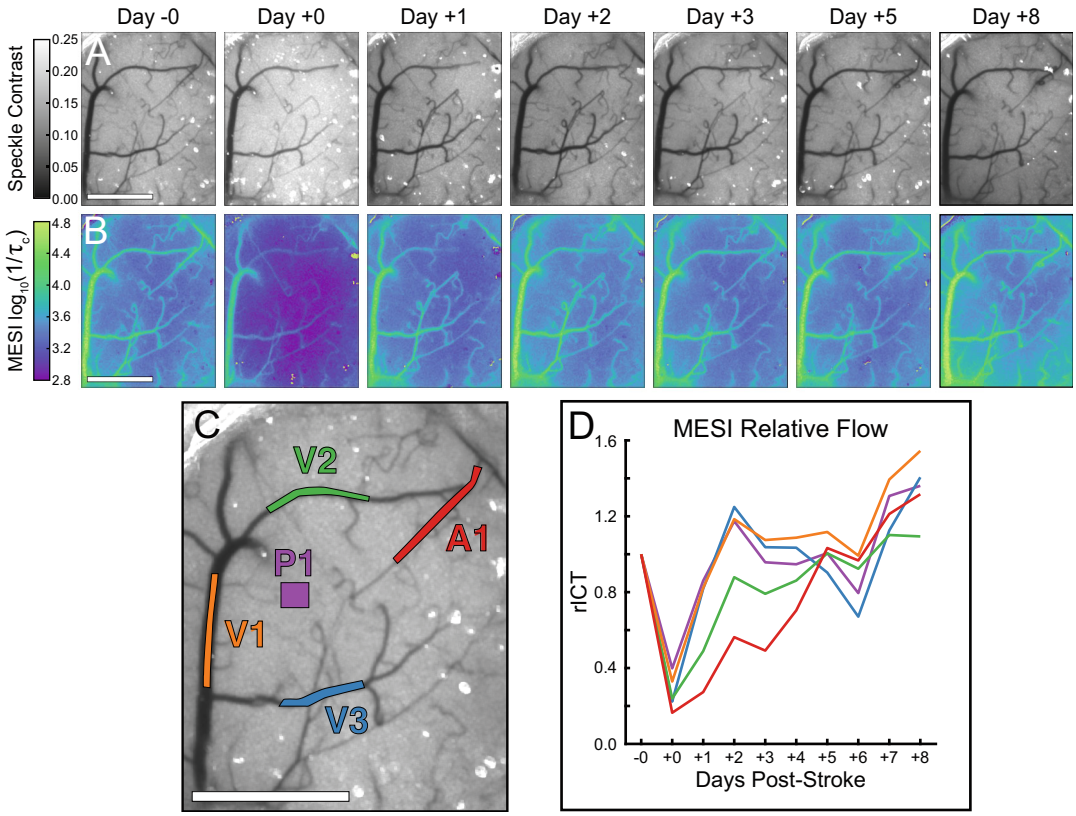

Fig. 4 Progression of the ischemic lesion over 8 days as imaged with (**a**) single-exposure LSCI displaying the speckle contrast images and (**b**) MESI displaying the ICT images on a log scale. Day −0 measurements were taken immediately prior to photothrombosis induction and Day +0 measurements were taken immediately after. (**c**) One arteriole (A1), three veins (V1), and one parenchyma region (P1) were targeted for chronic (**d**) relative blood flow. Relative MESI ICT was baselined against Day −0 measurements (White scale bars = 1 mm)

6. Convert the collected MESI data to ICT maps. This is done by solving for τ_c at every pixel in the image. As MESI allows for repeatable τ_c measurements across imaging sessions, we can reliably analyze and compare chronic changes in flow. Thus, we are able to monitor the progression and recovery of the ischemic lesion. In Fig. 4 we demonstrate the ability to use MESI to chronically monitor (over 8 consecutive days) the progression of an ischemic lesion, assess recovery of the vasculature, and the changes in relative blood flow pre- and post-stroke. The figure details are described as follows:

   (i) The perfusion of the occluded arteriole and broader effects on cortical flow were tracked using 5 ms single-exposure LSCI (Fig. 4a) and MESI ICT (Fig. 4b). The gradient between the occluded vessel and the surrounding tissue diminishes over the course of Days +1, +2, and +3 as

the occluded arteriole begins to reperfuse. By Day +5, the vessel had fully reperfused leaving little evidence of the infarct in the speckle contrast or ICT imagery.

(ii) The same five regions (one arteriole, three veins, and one parenchyma) used during the acute awake photothrombosis measurements were also targeted for chronic relative blood flow measurements (Fig. 4c, d). The relative blood flow was calculated using the pre-stroke (Day −0) MESI ICT measurements as the baseline. The first post-stroke measurements (Day +0) were taken immediately after the conclusion of the photothrombosis induction and reveal systemic deficits in blood flow, likely caused by the spreading depolarization. Blood flow within the targeted arteriole (A1) and a nearby vein (V2) slowly recovered over the course of 5 days while the remaining ROIs experienced a slight overshoot in relative flow during the same period. Flow continued to increase across all ROIs over the remaining 3 days and was elevated over baseline by the final imaging session on Day +8.

(iii) The speed of the recovery from the photothrombotic infarct is similar to the anesthetized [20, 41] with a full recovery after 5 days. The targeted arteriole remained occluded for 3 days following photothrombosis before fully reperfusing. During this period, another arteriole approaching from midline (bottom of the camera FOV) hyperperfused and likely served as a collateral blood supply to mitigate the severity of the flow deficit. Once flow was restored to the targeted vessel on Day +4, the collateral arteriole returned to near baseline flow.

4 Notes

1. Animals were allowed to recover from anesthesia and monitored for cranial window integrity and normal behavior for at least 2 weeks prior to imaging. Additional carprofen injections (5 mg/kg) were administered subcutaneously 2, 4, and 7 days post-surgery to relieve inflammation from the procedure. Cranial windows were lightly cleaned prior to each imaging session using a cotton swab and 70% ethanol (v/v). If necessary, a topical application of mineral oil was used to improve image quality by index matching. Any discoloration on or around the cranial window was documented and monitored for possible infection. Any cracks in or breaking of the cranial window were also documented and resulted in the immediate euthanasia of the animal.

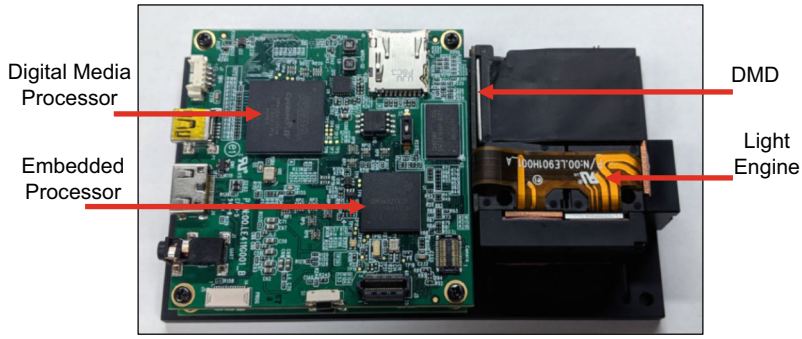

Fig. 5 Overview of TI DLP® LightCrafter™, indicating the four primary components that make up the evaluation board

2. Treadmill general maintenance tips: Thoroughly clean the surface of the wheel with 70% EtOH or a laboratory cleaner of your choice after removing the mouse from the wheel. Clean the area around the foam wheel. Urine and feces are sprayed off of the wheel when the mouse runs. It can be helpful to lay a paper towel or other disposable materials underneath the wheel to collect the majority of the mouse's waste. All parts should be free of oil, grease, or any other contaminants.
3. The Texas Instruments DLP® LightCrafter™ evaluation module contains a DLP3000 DMD, a DM365 embedded processor running Linux, and an RGB LED light engine developed by Young Optics, shown in Fig. 5. In order to utilize a custom light source such as a laser, the light engine must be removed to gain physical access to the DMD.
4. Further details about the MESI optical setup, necessary control electronics, and the required software packages and logic control can be found in a *Methods* paper form our lab [42] and in [20].
5. Despite the efficacy of the head restraint system, correlation time estimates with LSCI remain extremely sensitive to any motion within the imaging area. The animal walking would cause abrupt spikes in ICT that could not definitively be ascribed to neurovascular coupling instead of just a slight motion-related displacement. Excluding data during these periods of heightened activity offers the simplest solution for acquiring reliable instantaneous measurements of blood flow. However, if the hemodynamic response itself is being studied, then further measures would need to be taken in order to more robustly restrict motion of the brain.
6. The Speckle Software was modified to control the DMD via its Ethernet-over-USB command interface. Users can define arbitrarily shaped regions of interest (ROIs) using the LSCI camera as reference and upload the resulting binary masks to the DMD

for the patterning of excitation light. Registration between the camera and the projected pattern can be performed to guarantee alignment with the reference image. Individual patterns or timed pattern sequences can be uploaded and displayed on the DMD, with a TTL pulse emitted on each pattern change.

7. Animals were checked daily to monitor both behavior and the integrity of the cranial window by veterinary staff at the University of Texas at Austin Animal Research Center (ARC). Animals were housed in climate-controlled rooms with timed lighting (12-h light/dark cycles) to maintain a comfortable living environment and given food and water ad libitum. Social housing with multiple animals reduced the risk of overeating commonly seen when solo housing animals. This minimized possible growth in the animal's size and helped maintain the integrity of the cranial window. Any aggression resulted in the removal of the aggressor into a separate cage.

References

1. Janssen BJ, De Celle T, Debets JJ, Brouns AE, Callahan MF, Smith TL (2004) Effects of anesthetics on systemic hemodynamics in mice. Am J Phys Heart Circ Phys 287(4):H1618–H1624
2. Berg-Johnsen J, Langmoen IA (1992) The effect of isoflurane on excitatory synaptic transmission in the rat hippocampus. Acta Anaesthesiol Scand 36(4):350–355
3. Aksenov D, Eassa JE, Lakhoo J, Wyrwicz A, Linsenmeier RA (2012) Effect of isoflurane on brain tissue oxygen tension and cerebral autoregulation in rabbits. Neurosci Lett 524(2): 116–118
4. Pisauro MA, Dhruv NT, Carandini M, Benucci A (2013) Fast hemodynamic responses in the visual cortex of the awake mouse. J Neurosci 33(46):18343–18351
5. Strebel S, Lam A, Matta B, Mayberg TS, Aaslid R, Newell DW (1995) Dynamic and static cerebral autoregulation during isoflurane, desflurane, and propofol anesthesia. Anesthesiology 83(1):66–76
6. Iida H, Ohata H, Iida M, Watanabe Y, Dohi S (1998) Isoflurane and sevoflurane induce vasodilation of cerebral vessels via ATP-sensitive K+ channel activation. Anesthesiology 89(4): 954–960
7. Sakai H, Sheng H, Yates RB, Ishida K, Pearlstein RD, Warner DS (2007) Isoflurane provides long-term protection against focal cerebral ischemia in the rat. Anesthesiology 106(1):92–99
8. Burchell SR, Dixon BJ, Tang J, Zhang JH (2013) Isoflurane provides neuroprotection in neonatal hypoxic ischemic brain injury. J Investig Med 61(7):1078–1083
9. Schrandt CJ, Kazmi SS, Jones TA, Dunn AK (2015) Chronic monitoring of vascular progression after ischemic stroke using multiexposure speckle imaging and two-photon fluorescence microscopy. J Cereb Blood Flow Metab 35(6):933–942
10. Kapinya KJ, Prass K, Dirnagl U (2002) Isoflurane induced prolonged protection against cerebral ischemia in mice: a redox sensitive mechanism? Neuroreport 13(11):1431–1435
11. Seto A, Taylor S, Trudeau D, Swan I, Leung J, Reeson P, Brown CE (2014) Induction of ischemic stroke in awake freely moving mice reveals that isoflurane anesthesia can mask the benefits of a neuroprotection therapy. Front Neuroenerg 6:1
12. Kazmi SS, Salvaggio AJ, Estrada AD, Hemati MA, Shaydyuk NK, Roussakis E et al (2013) Three-dimensional mapping of oxygen tension in cortical arterioles before and after occlusion. Biomed Opt Express 4(7):1061–1073
13. Ponticorvo A, Dunn AK (2010) Simultaneous imaging of oxygen tension and blood flow in animals using a digital micromirror device. Opt Express 18(8):8160–8170
14. Sullender CT, Mark AE, Clark TA, Esipova TV, Vinogradov SA, Jones TA, Dunn AK (2018) Imaging of cortical oxygen tension and blood flow following targeted photothrombotic stroke. Neurophotonics 5(3):035003

15. Boas DA, Dunn AK (2010) Laser speckle contrast imaging in biomedical optics. J Biomed Opt 15(1):011109
16. Dunn AK (2012) Laser speckle contrast imaging of cerebral blood flow. Ann Biomed Eng 40(2):367–377
17. Dunn AK, Bolay H, Moskowitz MA, Boas DA (2001) Dynamic imaging of cerebral blood flow using laser speckle. J Cereb Blood Flow Metab 21(3):195–201
18. He F, Sullender CT, Zhu H, Williamson MR, Li X, Zhao Z, Luan L (2020) Multimodal mapping of neural activity and cerebral blood flow reveals long-lasting neurovascular dissociations after small-scale strokes. Sci Adv 6(21):eaba1933
19. Kazmi SMS, Parthasarthy AB, Song NE, Jones TA, Dunn AK (2013) Chronic imaging of cortical blood flow using multi-exposure speckle imaging. J Cereb Blood Flow Metab 33(6): 798–808
20. Sullender CT, Richards LM, He F, Luan L, Dunn AK (2022) Dynamics of isoflurane-induced vasodilation and blood flow of cerebral vasculature revealed by multi-exposure speckle imaging. J Neurosci Methods 366:109434
21. Soleimanzad H, Gurden H, Pain F (2018) Wide-field speckle imaging and two-photon microscopy for the investigation of cerebral blood flow in vivo in mice models of obesity. In: Biophotonics: photonic solutions for better health care VI, vol 10685. International Society for Optics and Photonics, p 1068508
22. Miller DR, Ashour R, Sullender CT, Dunn A (2021) Laser speckle contrast imaging for visualizing blood flow during cerebral aneurysm surgery: a comparison with indocyanine green angiography. medRxiv. https://doi.org/10.1101/2021.04.29.21254954
23. Richards LM, Kazmi SS, Olin KE, Waldron JS, Fox DJ Jr, Dunn AK (2017) Intraoperative multi-exposure speckle imaging of cerebral blood flow. J Cereb Blood Flow Metab 37(9): 3097–3109
24. Sicard KM, Fisher M (2009) Animal models of focal brain ischemia. Exp Transl Stroke Med 1: 1–6
25. Kozuimi J, Yoshida Y, Nakazawa T, Ooneda G (1986) Experimental studies of ischemic brain edema. 1. A new experimental model of cerebral embolism in rats in which recirculation can be introduced in the ischemic area. Jpn J Stroke 8:1–8
26. Carmichael ST (2005) Rodent models of focal stroke: size, mechanism, and purpose. NeuroRx 2(3):396–409
27. Brott T, Marler JR, Olinger CP, Adams HP Jr, Tomsick T, Barsan WG et al (1989) Measurements of acute cerebral infarction: lesion size by computed tomography. Stroke 20(7): 871–875
28. Watson BD, Dietrich WD, Busto R, Wachtel MS, Ginsberg MD (1985) Induction of reproducible brain infarction by photochemically initiated thrombosis. Ann Neurol 17(5): 497–504
29. Dietrich WD, Watson BD, Busto R, Ginsberg MD, Bethea JR (1987) Photochemically induced cerebral infarction: I. Early microvascular alterations. Acta Neuropathol 72(4): 315–325
30. Grome JJ, Gojowczyk G, Hofmann W, Graham DI (1988) Quantitation of photochemically induced focal cerebral ischemia in the rat. J Cereb Blood Flow Metab 8(1):89–95
31. Parthasarathy AB, Kazmi SS, Dunn AK (2010) Quantitative imaging of ischemic stroke through thinned skull in mice with multi exposure speckle imaging. Biomed Opt Express 1(1):246–259
32. Klaassen CD (1976) Pharmacokinetics of rose bengal in the rat, rabbit, dog, and guinea pig. Toxicol Appl Pharmacol 38(1):85–100
33. Gu W, Jiang W, Brännström T, Wester P (1999) Long-term cortical CBF recording by laser-Doppler flowmetry in awake freely moving rats subjected to reversible photothrombotic stroke. J Neurosci Methods 90(1):23–32
34. Helmchen F, Fee MS, Tank DW, Denk W (2001) A miniature head-mounted two-photon microscope: high-resolution brain imaging in freely moving animals. Neuron 31(6): 903–912
35. Flusberg BA, Jung JC, Cocker ED, Anderson EP, Schnitzer MJ (2005) In vivo brain imaging using a portable 3.9 gram two-photon fluorescence microendoscope. Opt Lett 30(17): 2272–2274
36. Dombeck DA, Khabbaz AN, Collman F, Adelman TL, Tank DW (2007) Imaging large-scale neural activity with cellular resolution in awake, mobile mice. Neuron 56(1):43–57
37. Wienisch M, Blauvelt DG, Sato TF, Murthy VN (2012) Two-photon imaging of neural activity in awake, head-restrained mice. In: Neuronal network analysis: concepts and experimental approaches. Humana Press, pp 45–60
38. Kaifosh P, Lovett-Barron M, Turi GF, Reardon TR, Losonczy A (2013) Septo-hippocampal GABAergic signaling across multiple

modalities in awake mice. Nat Neurosci 16(9): 1182–1184

39. Heiney SA, Ohmae S, Kim OA, Medina JF (2018) Single-unit extracellular recording from the cerebellum during eyeblink conditioning in head-fixed mice. Neuromethods 134:39–71
40. Silasi G, Xiao D, Vanni MP, Chen AC, Murphy TH (2016) Intact skull chronic windows for mesoscopic wide-field imaging in awake mice. J Neurosci Methods 267:141–149
41. Royer S, Zemelman BV, Losonczy A, Kim J, Chance F, Magee JC, Buzsáki G (2012) Control of timing, rate and bursts of hippocampal place cells by dendritic and somatic inhibition. Nat Neurosci 15(5):769–775
42. Santorelli A, Sullender CT, Dunn AK (2023) Multi-exposure speckle imaging for quantitative evaluation of cortical blood flow. In: Karamyan VT, Stowe AM (eds) Neural repair. Methods in molecular biology, vol 2616. Humana Press, New York
43. Balbi M, Vanni MP, Silasi G, Sekino Y, Bolanos L, LeDue JM, Murphy TH (2017) Targeted ischemic stroke induction and mesoscopic imaging assessment of blood flow and ischemic depolarization in awake mice. Neurophotonics 4(3):035001